

# Double Roles of Stabilization and Destabilization of Initiator Potassium Persulfate in Surfactant-Free Emulsion Polymerization of Styrene under Microwave Irradiation<sup>†</sup>

To Ngai<sup>‡</sup> and Chi Wu<sup>\*,‡,§</sup>

Department of Chemistry, The Chinese University of Hong Kong, Shatin, NT, Hong Kong, and  
The Open Laboratory of Bond Selection Chemistry, Department of Chemical Physics,  
The University of Science and Technology of China, Hefei, Anhui, 241000,  
People's Republic of China

Received March 11, 2005. In Final Form: June 19, 2005

Emulsifier-free emulsion polymerization of styrene in a water/acetone mixture under microwave irradiation resulted in narrowly distributed stable polystyrene nanoparticles with an averaged hydrodynamic radius ( $\langle R_h \rangle$ ) down to 35 nm when 50 wt % of acetone was added. For a given initiator potassium persulfate (KPS) concentration,  $\langle R_h \rangle$  was proportional to the monomer concentration in the range 1.2–7.0 wt %; while for a given monomer concentration,  $\langle R_h \rangle$  showed a minimum with an increasing initiator concentration. After both the roles of stabilization and destabilization of the initiator (KPS) were considered, we introduced a new parameter, the effective surface area stabilized per ionic group, and reformulated the Wu plot of  $\langle R_h \rangle \propto W_{\text{monomer}}/W_{\text{stabilizer}}$  into  $\langle R_h \rangle/[k_1(1 + k_2W_{\text{KPS}})] \propto W_{\text{monomer}}/W_{\text{initiator}}$ . It can qualitatively explain both the monomer and initiator concentration dependence of the particle size over a wide concentration range. The study of the salt effect showed that  $\langle R_h \rangle$  increased with the sodium sulfate concentration for fixed KPS and styrene concentrations.

## Introduction

The formulation and application of polymeric particles dispersed in a nonsolvent, such as latexes, have attracted much attention in academic and industrial researches for a long time.<sup>1–3</sup> Usually, emulsion, miniemulsion, and more recently, microemulsion are used to prepare these latexes.<sup>4,5</sup> Polymerization in oil-in-water (o/w) microemulsion has some advantages over emulsion polymerization because it can prepare transparent or translucent, stable, and monodisperse latex particles with a size 1 order of magnitude smaller than their counterparts produced with classical emulsion polymerization.<sup>6</sup> However, a drawback of the microemulsion polymerization is the addition of a large amount of surfactant required for the formulation. Such a high surfactant level is often not acceptable for economic or performance reasons. For example, it leaves unacceptable residues in products or constitutes contaminants in chemical reaction media, which has to be removed, resulting in a high cost.<sup>1,6,7</sup>

This is why emulsifier-free polymerization (EFP) has received much attention. The resultant colloidal particles are narrowly distributed in size with a “clean” surface and an excellent surface chemical feature, such as adhesion and water resistance.<sup>8,9</sup> Narrowly distributed latexes in the size range of 100 nm–5  $\mu\text{m}$  can be routinely prepared by such a method.<sup>10–12</sup> However, it is difficult to prepare surfactant-free polymeric particles in the size range of 10–100 nm with a high solid content because small particles have a strong tendency to coagulate with each other in a concentrated dispersion. Therefore, the preparation of stable surfactant-free polymeric nanoparticles with a high solid content is a long-standing challenge in polymeric colloidal research.

Generally, the stability of emulsifier-free latex particles produced via a persulfate initiation increases with the charge density and the hydrophilicity of the particle surface. Therefore, the following approaches are often adopted to improve the stability: (1) using a water-soluble initiator, (2) increasing the monomer solubility in the disperse medium, (3) copolymerizing hydrophobic monomer with another hydrophilic comonomer or surface-active functional comonomer, and (4) adding a water-soluble organic solvent into the aqueous phase.<sup>8</sup> According to the DLVO theory, the total pair interaction among colloidal particles consists of both the Coulombic and the van der Waals interaction. The two ionic groups generated from the decomposition of an initiator, such as persulfate, are chemically bonded to the polymer chain ends, presumably located on the particle surface. The existence of these ionic

<sup>†</sup> In the memory of the later Professor Wenming Zhang from Anhui Normal University, China.

\* To whom correspondence should be addressed. Telephone: +852-2609-6106. Fax: +852-2603-5057. E-mail: chiwu@cuhk.edu.hk.

<sup>‡</sup> The Chinese University of Hong Kong.

<sup>§</sup> The University of Science and Technology of China.

(1) Klier, J.; Tucker, C. J.; Kalantar, T. H.; Green, D. P. *Adv. Mater.* **2001**, *12*, 1751.

(2) *Emulsion Polymerization and Emulsion Polymers*; Lovell, P. A., El-Aasser, M. S., Eds.; Wiley: New York, 1997.

(3) Klier, J.; Strandburg, G. M.; Tucher, C. J. U.S. Patent 5 597 792, 1997.

(4) Choi, Y. T.; El-Aasser, M. S.; Sudol, E. D.; Vanderhoff, J. W. *J. Polym. Sci., Part A: Polym. Chem.* **1985**, *23*, 2973.

(5) Candau, F. In *Polymerization in Organized Media*; Paleos, C. M., Ed.; Gordon Breach Science: Philadelphia, PA, 1992; chapter 4.

(6) Gan, L. M.; Chew, C. H. In *The Polymeric Materials Encyclopedia*; Joseph, C., Ed.; CRC Press: Boca Raton, FL, 1996.

(7) Puig, J. E. In *The Polymeric Materials Encyclopedia*; Joseph, C., Ed.; CRC Press: Boca Raton, FL, 1996.

(8) Aslamazova, T. R. *Prog. Org. Coat.* **1995**, *25*, 109.

(9) Bataille, P.; Almassi, M.; Inoue, M. *J. Appl. Polym. Sci.* **1998**, *67*, 1711.

(10) Song, Z.; Poehlein, G. W. *J. Polym. Sci., Part A: Polym. Chem.* **1990**, *28*, 2359.

(11) Kotera, A.; Furusawa, K.; Takeda, Y.; Kolloid, Z. Z. *Polymer* **1970**, *239*, 677.

(12) Chiu, W.; Shih, C. *J. Appl. Polym. Sci.* **1986**, *31*, 2117.

groups affect not only the electrostatic stability but also the particle size.<sup>13,14</sup> On one hand, increasing the initiator concentration can promote the stability because more ionic groups acted as stabilizer are available.<sup>15</sup> On the other hand, the existence of these ionic groups and counterions increases the ionic strength and compresses the electrostatic double layer on the particle surface,<sup>16,17</sup> which decreases the particle stability.

We have established a simple scaling between the average radius of polymeric particles ( $R$ ) and the initial macroscopic monomer/surfactant weight ratio ( $W_{\text{monomer}}/W_{\text{surfactant}}$ ) for microemulsion polymerization, namely,<sup>18</sup>

$$sR \propto W_{\text{monomer}}/W_{\text{surfactant}} \quad (1)$$

where  $s$  is the average surface area occupied per surfactant molecule. For a given microemulsion, the ionic strength can be regarded as a constant because of the existence of a large amount of ionic surfactant. In contrast, the emulsifier-free emulsion polymerization contains no surfactant. In principle, we could still use eq 1 for emulsifier-free emulsion polymerization if considering  $W_{\text{surfactant}}$  as the weight of stabilizers, regardless of the nature of the stabilizer.

The emulsifier-free emulsion polymerization of styrene in a water/acetone mixture has been investigated before.<sup>19</sup> Acetone is miscible with water and styrene but a non-solvent for polystyrene. When the acetone content is lower than 40 v/v %, stable emulsion could be prepared and the polymerization rate was remarkably increased in comparison with the one in pure water. Fitch<sup>13</sup> proposed that the number of the particles increases with an increasing initiation rate but decreases with an increasing radical capture rate. They found that the particle size decreased from 0.5 to 0.17  $\mu\text{m}$  when the acetone content increased from 0 to 40 v/v %. In this study, to prepare emulsifier-free narrowly distributed polymeric latex particles, the mixed solvent–irradiation method was combined with the novel microwave–irradiation method recently developed in our laboratory.<sup>20</sup>

## Experimental Procedures

**Sample Preparation.** Styrene monomer was purified by a standard procedure.<sup>21</sup> Analytical-grade potassium persulfate (KPS, from Merck), acetone, and sodium chloride were used without further purification. Deionized water from a Millipore Nanopure water system with a resistivity of 18 M $\Omega$  cm was used in all of the experiments.

The different recipes used for preparation of polystyrene particles are summarized in Table 1. A modified domestic microwave oven (Whirlpool-Vip 20) with a double emission at 2450 MHz and a maximum output power of 900 W was used. A 250-mL four-neck flask was assembled inside the oven. The center neck was connected with a water reflux condenser and a coaxial glass stirrer. The other three necks were used for a nitrogen inlet, an *in situ* sample drawing, and an inserted thermometer, respectively. The reaction mixture (150 g) with a proper composition was weighted in the flask and was bubbled with nitrogen for  $\sim$ 30 min at room temperature. The reaction mixture

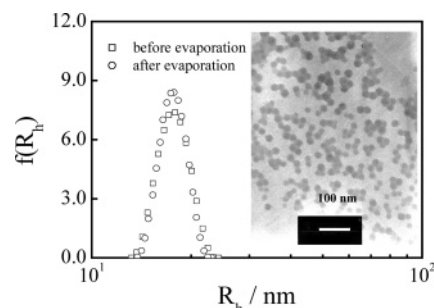


**Figure 1.** Typical hydrodynamic radius distribution  $f(R_h)$  of the resultant nanoparticles prepared by surfactant-free emulsion copolymerization in a water/acetone (50:50 weight ratio) mixture under microwave irradiation. The inset shows the TEM micrograph of the nanoparticles.

**Table 1. Polymerization Recipes for Synthesis of Polystyrene Particles**

$W_{\text{acetone}}/(W_{\text{acetone}} + W_{\text{water}})$	$C_{\text{styrene}}$ (g/mL)	$C_{\text{KPS}}$ (g/mL)
0.1	$3.38 \times 10^{-2}$	$2.39 \times 10^{-3}$
0.2	$3.38 \times 10^{-2}$	$2.39 \times 10^{-3}$
0.3	$3.38 \times 10^{-2}$	$2.39 \times 10^{-3}$
0.4	$3.38 \times 10^{-2}$	$2.39 \times 10^{-3}$
0.5	$3.38 \times 10^{-2}$	$2.39 \times 10^{-3}$
0.6	$3.38 \times 10^{-2}$	$2.39 \times 10^{-3}$
0.5	$1.07 \times 10^{-2}$	$2.39 \times 10^{-3}$
0.5	$1.60 \times 10^{-2}$	$2.39 \times 10^{-3}$
0.5	$3.38 \times 10^{-2}$	$2.39 \times 10^{-3}$
0.5	$4.01 \times 10^{-2}$	$2.39 \times 10^{-3}$
0.5	$5.60 \times 10^{-2}$	$2.39 \times 10^{-3}$
0.5	$1.60 \times 10^{-2}$	$2.36 \times 10^{-4}$
0.5	$1.60 \times 10^{-2}$	$2.94 \times 10^{-4}$
0.5	$1.60 \times 10^{-2}$	$4.01 \times 10^{-4}$
0.5	$1.60 \times 10^{-2}$	$8.05 \times 10^{-4}$
0.5	$1.60 \times 10^{-2}$	$1.60 \times 10^{-3}$
0.5	$1.60 \times 10^{-2}$	$2.39 \times 10^{-3}$

was then exposed to the microwave irradiation to start the polymerization. The stirring speed was kept at  $\sim$ 300 rpm. The reaction temperature ( $63 \pm 1$  °C) was reached within 2 min and maintained by adjusting the microwave power.

A small amount of the dispersion was collected at different reaction stages. Parts of the collected sample ( $\sim$ 0.02 g) were diluted immediately with cold deionized water ( $\sim$ 20.0 mL) to stop the reaction. A few drops of sodium chloride solution were added to screen out the long-range electrostatic interaction before laser light-scattering measurement. The sodium chloride concentration was kept so low (0.01 M) that no effect on the resultant particles was observed even after a long time. The rest of the collected sample was dried and weighed, which led to the polymerization yield at different reaction stages.

**Laser Light Scattering.** A modified commercial spectrometer (ALV/SP-125) equipped with a multi- $\tau$  digital time correlator (ALV-5000) and a solid-state laser (ADLAS DPY425II, output power  $\sim$  400 mW at  $\lambda_0 = 532$  nm) was used. The beam was properly attenuated. The principle of LLS can be found elsewhere.<sup>22</sup> In dynamic LLS, the Laplace analysis of the measured time correlation function leads to the hydrodynamic radius distribution ( $f(R_h)$ ). In this study, all of the LLS measurements were conducted at  $25.0 \pm 0.1$  °C.

## Results and Discussion

In Figure 1, both dynamic laser light-scattering and transmission electron microscopy results reveal that the particles prepared in the water/acetone mixture are not only small but also narrowly distributed. Figure 1 also shows that the removal of acetone from the resultant dispersion by vacuum distillation has no effect on the particle size distribution. Note that no surfactant was

(13) Fitch, R. M. *Br. J. Polym.* **1973**, *5*, 467.

(14) Kawaguchi, H.; Sugi, Y.; Ohtsuka, Y. *J. Appl. Polym. Sci.* **1981**, *26*, 1649.

(15) Ohtsuka, Y.; Kawaguchi, H.; Sugi, Y. *J. Appl. Polym. Sci.* **1981**, *26*, 1637.

(16) Chu, X.; Wasan, D. T. *J. Colloid Interface Science* **1996**, *184*, 268.

(17) Sakota, K.; Okaya, T. *J. Appl. Polym. Sci.* **1977**, *21*, 1025.

(18) Wu, C. *Macromolecules* **1994**, *27*, 298–299.

(19) Okubo, M.; Yamada, A.; Shibao, S. et al. *J. Appl. Polym. Sci.* **1981**, *26*, 1675–1679.

(20) Zhang, W.; Gao, J.; Wu, C. *Macromolecules* **1997**, *30*, 6388.

(21) Zhang, W.; Wu, C. *Acta Phys. Chim. Sin.* **1993**, *9*, 1.

(22) Berne, B.; Pecora, R. *Dynamic Light Scattering*, Plenum Press: New York, 1976.

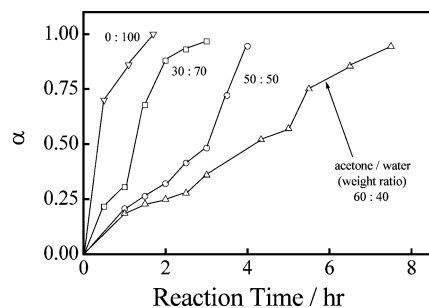


**Figure 2.** Solvent composition dependence on the conversion rate of styrene in the surfactant-free emulsion polymerization under microwave irradiation, where the amount of styrene and KPS in the polymerization are  $3.38 \times 10^{-2}$  and  $2.39 \times 10^{-3}$  g/mL, respectively.

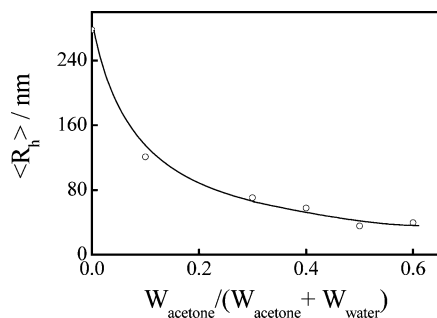


**Figure 3.** Solvent composition dependence on the average hydrodynamic radius of the nanoparticles prepared by surfactant-free polymerization under microwave irradiation, where the amount of styrene and KPS in the polymerization are  $3.38 \times 10^{-2}$  and  $2.39 \times 10^{-3}$  g/mL, respectively.

added in the dispersion and that the resulted particles are stable because there was no change of the particle size distribution for several months. To investigate the effects of the composition (the water/acetone ratio) as well as the absolute monomer and the initial KPS concentrations on the size distribution of the resultant polymeric particles, a series of emulsifier-free emulsion polymerization reactions were conducted.

Figure 2 shows that, under the microwave irradiation, the rate of polymerization decreases with an increasing acetone content, contradicting the results reported by Okubo et al.<sup>19</sup> for the surfactant-free emulsion polymerization of styrene under conventional heating. They found that the conversion rate increased with an increasing acetone content below  $\sim 40$  v/v %, which was attributed to the stability of both styrene and oligomeric radicals. In our case, only water molecules were “heated” by microwave. Therefore, the heating efficiency decreases with the water content. This explains why the conversion rate decreases with an increasing acetone content. However, it should be noted that, for the same acetone content, the microwave irradiation always leads to a faster conversion rate than conventional heating. This is because the decomposition rate of the initiator, KPS, under the microwave irradiation is faster than that under conventional heating, which shortens the induction period of the polymerization and results in a faster reaction rate.<sup>23,24</sup>

Figure 3 shows the decrease of the particle size with an increasing acetone content up to  $\sim 50$  wt %. The same tendency was also reported for the surfactant-free emulsion polymerization of styrene in a water/methanol mixture as well as in a water/acetone mixture.<sup>19,25</sup> Homola

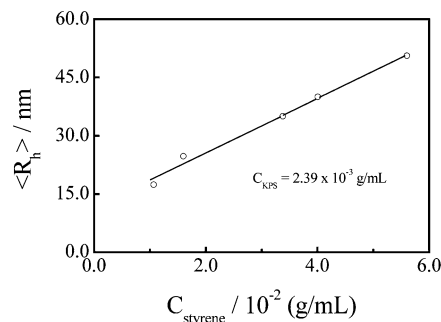


**Figure 4.** Styrene concentration dependence of the average hydrodynamic radius  $\langle R_h \rangle$  of the nanoparticles prepared by surfactant-free polymerization under microwave irradiation, where the KPS concentration ( $C_{\text{KPS}}$ ) and acetone content are fixed at  $2.39 \times 10^{-3}$  g/mL and 50 wt %, respectively.

et al.<sup>25</sup> showed a small decrease of the particle size from 0.6 to 0.5  $\mu\text{m}$  as the methanol content increased from 0 to 100 v/v %, whereas Okubo et al.<sup>19</sup> reported a decrease of the particle size from 0.5 to 0.17  $\mu\text{m}$  as the acetone content increased from 0 to 40 v/v %.

Our results reveal that under the microwave irradiation, the particle size decreases greatly down to  $\sim 70$  nm when the acetone content is 50 wt %. Also note in Figure 3 that the addition of only 10 wt % acetone in water results in a sharp decrease of  $\langle R_h \rangle$  from 278 to 121 nm. The reason can be partially attributed to the fact that the presence of acetone reduces the surface tension during the polymerization, leading to the formation of smaller particles. A further increase of the acetone content led to a linear decrease of  $\langle R_h \rangle$ . When the acetone content is higher than 50 wt %, the particle size starts to increase and the size distribution becomes broader, which can be attributed to the particle nucleation at the initial stage.<sup>19</sup>

Figure 4 shows that the average hydrodynamic radius  $\langle R_h \rangle$  of the resultant particles is a linear function of the monomer concentration, similar to the case of the emulsion polymerization of styrene in the presence of the surfactant under the microwave irradiation.<sup>18</sup> Considering the ionic groups generated by KPS as stabilizers, we can understand such a linear function because each stabilizer can occupy a certain area of the particle surface ( $s$ ) for a given dispersion.<sup>18</sup> For a given  $C_{\text{KPS}}$  (assuming a constant decomposition ratio), the total surface area stabilized should be constant. This explains why the addition of more monomers can increase the particle size because smaller particles have a larger total surface area, in which the surface area per stabilizer (ionic group) is kept constant.

On the other hand, Figure 5 shows the decrease of the average hydrodynamic radius  $\langle R_h \rangle$  of the resultant particles with an increasing KPS concentration in the range  $C_{\text{KPS}} \leq 8 \times 10^{-4}$  g/mL. It is understandable because, for a fixed monomer concentration ( $C_{\text{styrene}}$ ), more KPS molecules can generate more ionic groups and stabilize a larger total surface area so that  $\langle R_h \rangle$  decreases. A further increase of  $C_{\text{KPS}}$  results in an increase of  $\langle R_h \rangle$  because the decomposition of KPS also increases the ionic strength of the dispersion, which leads to a decrease of the average effective surface area, stabilized per ionic group. As  $C_{\text{KPS}}$  increases, the effect of ionic strength becomes dominant so that the particle size increases. A combination of Figures 4 and 5 show that  $\langle R_h \rangle$  is a complicated function of the initial KPS concentrations as well as the ratio of  $C_{\text{styrene}}/C_{\text{KPS}}$ .

(23) Bao, J. J.; Zhang, A. M. *J. Appl. Polym. Sci.* **2004**, *93*, 2815.

(24) Xu, Z.-S.; Deng, Z.-W.; Hu, X.-X.; Li, L.; Yi, C.-F. *J. Polym. Sci., Part A: Polym. Chem.* **2005**, *43*, 2368.

(25) Homola, A. M.; Inoue, M.; Robertson, A. A. *J. Appl. Polym. Sci.* **1975**, *19*, 3077–3086.

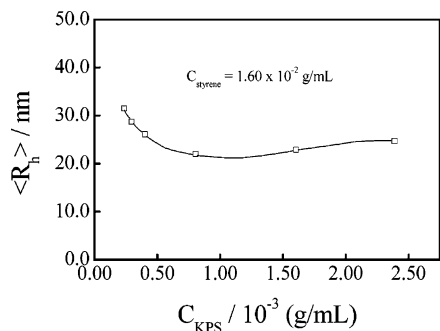


**Figure 5.** Initiator concentration dependence of the average hydrodynamic radius  $\langle R_h \rangle$  of the resultant polystyrene nanoparticles, where both the styrene concentration was kept at  $1.60 \times 10^{-2}$  g/mL and the acetone content was 50 wt %.

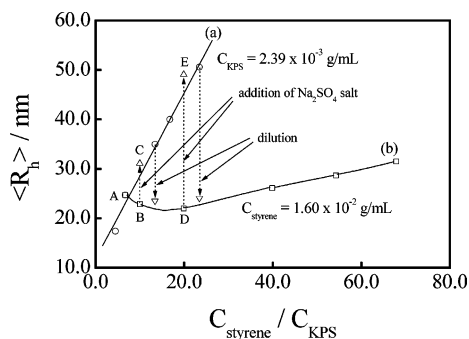


**Figure 6.** Fleet ratio ( $W_{styrene}/W_{KPS}$ ) dependence of the average hydrodynamic radius ( $R_h$ ) of the resultant polystyrene particles, where curve a is a replot curve from Figure 4 and b is a replot from Figure 5.

Figure 6 shows a replot of Figures 4 and 5. Note that, for curve b,  $C_{KPS}$  used is lower than  $2.39 \times 10^{-3}$  g/mL used in curve a. Also note that, for a given  $C_{styrene}/C_{KPS}$ , curve b has a smaller  $\langle R_h \rangle$  than line a. It is clear that the size of the resultant particles depends not only on the ratio of  $C_{styrene}/C_{KPS}$  but also on the initial KPS concentration. Therefore, we have to introduce an effective surface area ( $s$ ) per each KPS-generated ionic group. It has been known that the surfactant-free emulsion polymerization of styrene consists of two stages.<sup>10,26,27</sup> In the first stage, a large number of micelle-like oligomeric particles are generated. As the propagation continues, these oligomeric particles gradually lose their stability and undergo interparticle coagulation near the end of the first stage. The interparticle coagulation resulted from (1) the dramatic decrease of the charge density on the surface as individual polymer chains inside each particle become longer and (2) the increase of the surface/volume ratio. In the second stage, the number of particles decreases as a result of the initial interparticle coagulation. During such a process, the surface charge density gradually approaches a constant and becomes sufficiently high to prevent further coagulation. At this point,  $s = 4\pi R^2/n$ , where  $R$  and  $n$  are the average particle radius and the average number of polymer chains inside each stable particle, respectively. Further,  $n = N_A[(4/3)\pi R^3 \rho]/M_{chain}$ , where  $N_A$ ,  $\rho$ , and  $M_{chain}$  are Avogadro's constant, the average particle density, and the average molar mass of the polymer chains inside each particle, respectively. In this case, we have assumed that each polymer chain within a given polymer particle carries only one charge. Note that  $M_{chain}$  is proportional to the Fleet ratio ( $W_{monomer}/W_{initiator}$ ). Thus,  $sR \propto W_{monomer}/W_{initiator}$ , identical to eq 1 if we only consider the short chains with

ionic groups as stabilizers but not their contribution to the ionic strength.

However, a variation of the initiator concentration affects ionic strength ( $I$ ). The increase of the ionic strength reduces the electrostatic repulsion among the ionic groups so that the effective surface area stabilized per ionic group decreases; namely,  $s$  becomes smaller. It is easy to understand that those ionic groups from KPS, on one hand, act as stabilizers but on the other hand, at the same time, become destabilizers. It is well-known that the Debye length ( $l_D$ ) is proportional to  $I^{-1/2}$ ; namely,  $l_D^2 \propto 1/I \propto 1/W_{initiator}$ . Therefore, the effective surface area ( $s$ ) per ionic group should be proportional to  $l_D^2$ , i.e.,  $s \propto s_0/(1 + kI)$ , where  $k$  is a constant and  $s_0$  is the surface area stabilized per ionic group at  $I \rightarrow 0$ . Considering the two opposite effects (stabilizer and destabilizer), we can rewrite eq 1 as

$$\frac{R}{s(1 + kI)} = \frac{W_{monomer}}{W_{initiator}} + k' \quad (2)$$

where  $s$ ,  $k$ , and  $k'$  are constants. Equation 2 shows that, when the KPS (initiator) concentration is low, the stabilization effect is dominant so that the particle size decreases with an increasing KPS concentration; while as the KPS concentration increases, the destabilization effect becomes dominant so that the particle size increases with the KPS concentration. Our previous study showed that, for a given monomer concentration,  $\langle R_h \rangle$  linearly increases with  $C_{KPS}$ ,<sup>20</sup> i.e.,  $\langle R_h \rangle \propto C_{KPS}$ . Recently, Peach et al. also found that  $\langle R_h \rangle$  increases with an increasing  $C_{KPS}$ . Considering that  $I \propto W_{initiator}$ , we can rewrite eq 2 as

$$R = s \frac{W_{monomer}}{W_{initiator}} + skW_{monomer} + skk'W_{initiator} + sk' \quad (3)$$

For a given  $W_{monomer}$ , eq 3 predicts that  $R \propto W_{initiator}$  when the KPS concentration is sufficiently higher but  $R \propto 1/W_{initiator}$  when the KPS concentration is low. On the other hand,  $R$  is proportional to  $W_{monomer}$  for a given KPS concentration, as already shown in Figure 4.

To prove what has been discussed, we chose two compositions (points B and D in Figure 6) and adjust the ionic strength by adding a proper amount of sodium sulfate so that their ionic strengths become identical as those used in the straight line. We found that the average hydrodynamic radius of resultant particles increases to C and E, respectively, clearly demonstrating that the ionic strength can influence the particle size. Therefore, to synthesize small particles, we should keep the ionic strength of the dispersion media as low as possible. The addition of acetone lowers the ionic strength so that the resultant particles are smaller in comparison with those obtained in pure water. Our results suggest that we can control the particle size simply by adjusting the ionic strength of the initial reaction mixture. Figure 6 also shows that, for a given  $C_{styrene}/C_{KPS}$ , we can push curve AC to curve AB by adding a proper amount of water to make the initial KPS concentration of the reaction mixture identical to those on curve AB. It can be seen that the values of  $\langle R_h \rangle$  for the two points with higher salt concentrations can be pushed down after dilution. In these cases, the values of  $\langle R_h \rangle$  after dilution are close to those on curve AC because the dilution decreases the ionic concentration ( $I$ ).

Figure 7 shows the Fleet ratio  $W_{monomer}/W_{initiator}$  (here, it is  $W_{styrene}/W_{KPS}$ ) dependence of the average hydrodynamic radius ( $R_h$ ) at three different initial KPS concentrations.

(26) Tauer, K. *Macromolecules* **1998**, *31*, 9390.

(27) Peach, S. *Macromolecules* **1998**, *31*, 3372–3373.

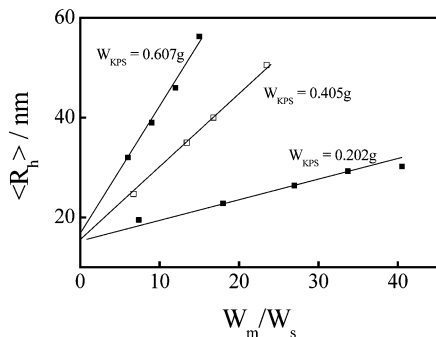


**Figure 7.** Fleet ratio ( $W_{\text{styrene}}/W_{\text{KPS}}$ ) dependence of the average hydrodynamic radius ( $\langle R_h \rangle$ ) of the resultant polystyrene nanoparticles for three initial KPS concentrations, where curve AC corresponds to that in Figure 6.

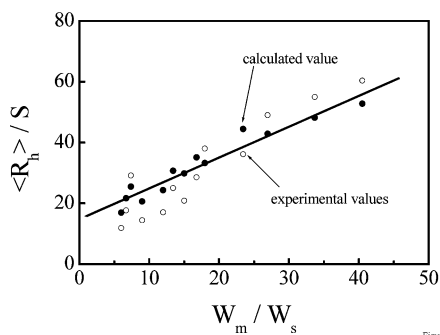


Figure 8(C)

**Figure 8.** Replot showing the Fleet ratio ( $W_{\text{styrene}}/W_{\text{KPS}}$ ) dependence of the average hydrodynamic radius ( $\langle R_h \rangle$ ) of the synthesized polystyrene nanoparticles via microwave irradiation. ● and ○ represent the calculated and experimental ( $\langle R_h \rangle/k_1$ ) values, respectively.

It is clear that  $\langle R_h \rangle$  is proportional to the Fleet ratio for each given  $C_{\text{KPS}}$ . It can be seen that the y intercepts of these three lines slightly increase with the initial KPS concentration, which is expected from eq 3. Furthermore, for a given Fleet ratio, we can rewrite eq 3 as

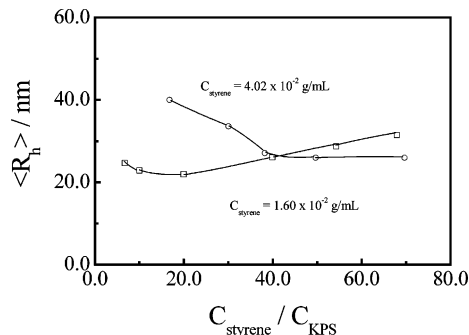
$$R = s \frac{W_{\text{monomer}}}{W_{\text{initiator}}} + \left( sk \frac{W_{\text{monomer}}}{W_{\text{initiator}}} + skk' \right) W_{\text{initiator}} + sk' \quad (4)$$

This is why  $\langle R_h \rangle$  increases with the initiator concentration ( $C_{\text{KPS}}$ ) for a fixed ratio of  $W_{\text{monomer}}/W_{\text{initiator}}$ . It is helpful to note that the slopes of the three lines in Figure 7 increase with the initial KPS concentrations, which contradict eq 4 if we assume that the average surface area per ionic group ( $s$ ) is a constant. Therefore, we have to modify the ionic strength dependence of  $s$  in the high initiator concentration range as

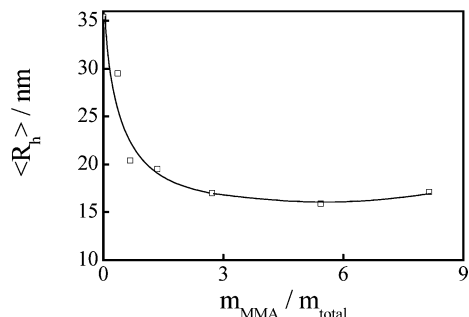
$$s = s_0 \exp(-k W_{\text{initiator}}) \quad (5)$$

Figure 8 shows a replot of the Fleet ratio dependence of the average hydrodynamic radius ( $\langle R_h \rangle$ ) at three initial KPS concentrations after we considered the effective average surface area per ionic group. Also note that the ratios of  $\langle R_h \rangle/s$  calculated from the initial KPS concentrations agree well with those experimental values. They converge into a straight line. Figure 8 further supports that the average hydrodynamic radius ( $\langle R_h \rangle$ ) of the resultant particles under microwave irradiation can be predicted from a combination of eqs 4 and 5.

Further, Figure 9 shows how the particle size depends on the Fleet ratio for two different initial styrene concentrations. It can also be qualitatively explained on



**Figure 9.** Fleet ratio ( $W_{\text{styrene}}/W_{\text{KPS}}$ ) dependence of the average hydrodynamic radius ( $\langle R_h \rangle$ ) of the resultant polystyrene nanoparticles for two initial styrene concentrations.



**Figure 10.** Plot showing the effect of methyl methacrylate (MMA) content on the hydrodynamic radius ( $\langle R_h \rangle$ ) of the synthesized copolymer nanoparticles.

the basis of eq 3. In the case of  $C_{\text{styrene}} = 4.02 \times 10^{-2} \text{g/mL}$ , the particle size does not change too much with an increasing  $C_{\text{KPS}}$  (and decreasing  $C_{\text{styrene}}/C_{\text{KPS}}$ ) until  $C_{\text{KPS}}$  reaches a certain value. Note that, in this case, the monomer concentration is so high that the second right term of eq 3 is dominant. On the other hand, the effects of the first and third right terms of eq 3 have the opposite trends when  $W_{\text{initiator}}$  is not too high. This is why the initial increase of  $C_{\text{KPS}}$  has nearly no effect on the particle size in the range  $C_{\text{styrene}}/C_{\text{KPS}} > 40$ .

Figure 10 reveals the effect of the composition of the monomers on the size of the resultant particles, where  $m_{\text{MMA}}$  and  $m_{\text{styrene}}$  are the masses of methyl methacrylate and styrene used, respectively. Both the solvent composition and the initiator amount are fixed as those in Figure 5, i.e.,  $m_{\text{acetone}}/m_{\text{water}} = 1.0$  and  $m_{\text{KPS}} = 0.4060 \pm 0.0005 \text{g}$ . For  $m_{\text{MMA}}/m_{\text{styrene}} = 0$ ,  $\langle R_h \rangle = 35.0 \text{nm}$ . The particle size significantly decreases to 20.0 nm with the addition of a small amount of MMA. It indicates that MMA in this reaction acts not only as comonomer but also as a kind of stabilizer. However, a further increase of the MMA content does not have too much of an effect on the particle size. It should also be noted that such resultant particles are also very stable over a wide range of  $m_{\text{MMA}}/m_{\text{styrene}}$ . Considering that MMA is more soluble in water, we can explain the MMA effect as follows. When a small amount of MMA is added, the free radicals generated from KPS have a higher chance to react with MMA to form more chains with an ionic end in comparison with the case without the addition of MMA. The association of these chains leads to more particle seeds so that the final particles, on average, become smaller. This leads to a very convenient way to control the particle size.

## Conclusion

From a combination of the water/acetone mixture and the microwave irradiation, we are able to prepare narrowly

distributed small emulsifier-free polystyrene latex particles with good stability and reproducibility. After considering the stabilization and destabilization effect of the initiator (KPS) used, we can explain the effect of the Fleet ( $W_{\text{monomer}}/W_{\text{initiator}}$ ) ratio, monomer and initiator concentrations on the size of the resultant particles based on a previously established structural model. Our results showed that, by adjusting the initial ionic strength of the reaction mixture, one could control the particle size. On the other hand, the addition of a small amount of relatively more hydrophilic comonomer, such as MMA, can effectively decrease the size of the resultant particles, which provides an easy and convenient way to prepare small surfactant-free polymeric particles. This is because free

radicals generated from water-soluble initiator have a higher chance to react with the comonomer, which is more soluble in water to form more chains with an ionic end, and the association of these chains leads to more seeds for further polymerization. The effect is the same as the addition of organic solvent in water.

**Acknowledgment.** The financial support of the Hong Kong Special Administration Region Earmarked Grants (CUHK4025/02P, 2160181) and the National Natural Science Foundation (NNSF) of China (2003/2005, 20274045) is gratefully acknowledged.

LA0506630